

# 22 nm FD-SOI MOSFET Figures of Merit at high temperatures upto 175 °C

Arka Halder

*Institute of Information and  
Communication Technologies,  
Electronics and Applied  
Mathematics (ICTEAM)*  
Université catholique de Louvain  
Louvain-la-Neuve, Belgium  
arka.halder@uclouvain.be

Lucas Nyssens

*Institute of Information and  
Communication Technologies,  
Electronics and Applied  
Mathematics (ICTEAM)*  
Université catholique de Louvain  
Louvain-la-Neuve, Belgium  
lucas.nyssens@uclouvain.be

Martin Rack

*Institute of Information and  
Communication Technologies,  
Electronics and Applied  
Mathematics (ICTEAM)*  
Université catholique de Louvain  
Louvain-la-Neuve, Belgium  
martin.rack@uclouvain.be

Dimitri Lederer

*Institute of Information and  
Communication Technologies,  
Electronics and Applied  
Mathematics (ICTEAM)*  
Université catholique de Louvain  
Louvain-la-Neuve, Belgium  
dimitri.lederer@uclouvain.be

Valeriya Kilchytska

*Institute of Information and  
Communication Technologies,  
Electronics and Applied  
Mathematics (ICTEAM)*  
Université catholique de Louvain  
Louvain-la-Neuve, Belgium  
valeriya.kilchytska@uclouvain.be

Jean-Pierre Raskin

*Institute of Information and  
Communication Technologies,  
Electronics and Applied  
Mathematics (ICTEAM)*  
Université catholique de Louvain  
Louvain-la-Neuve, Belgium  
jean-pierre.raskin@uclouvain.be

**Abstract**— This work studies the impact of increase in temperature on the RF and analog figures of merit (FoMs) of 22 nm FD-SOI MOSFETs from room temperature of 25 °C to 175 °C. DC and RF measurements are performed on the MOSFETs to extract the main RF FoMs over temperature. From DC measurements in temperature, the zero-temperature coefficient (ZTC) point and threshold voltage ( $V_{Th}$ ) reduction on increasing temperature is observed. Through direct on-wafer RF measurements reductions of 21 % in the current-gain cut-off frequency ( $f_T$ ) and of 14 % in the maximum oscillation frequency ( $f_{max}$ ) are observed at 175 °C compared to 25 °C. In particular, the evolution over temperature of transconductance ( $g_m$ ) appears to be one of the major causes of the degradation in  $f_T$  and  $f_{max}$ .

**Keywords**— *FDSOI,  $f_T$ ,  $f_{max}$ , Figures of Merit (FoMs), high temperature*

## I. INTRODUCTION

22 nm FD-SOI technology from GlobalFoundries is a technology of choice for upcoming RF and high frequency applications. This technology targets a wide variety of applications ranging from IoT/wearables to automotive, millimetre wave radar, 5G communications, etc. The intrinsic  $f_T$  and  $f_{max}$  of NMOS devices in 22FDX technology are reported to be around 347 GHz and 371 GHz [1], demonstrating excellent results that enable RF and millimetre wave designs. The RF performance of MOSFETs can be evaluated by considering 2 main figures of merit (FoMs): cut-off frequency  $f_T$  and maximum oscillation frequency  $f_{max}$ . Previously, electronic circuitry exposed to high temperature applications was mainly limited, but this has now broadened to diverse applications. Circuits like automotive electronic circuits located close to the engine for

example, are subject to high temperature environment [2]. Additionally, the presence of self-heating in devices causes a rise in temperature simply due to Joule heating from device current during operation. These aforementioned factors motivate the need to observe and correctly quantify the effect of these increased temperatures on the performance of such circuits. In this paper, the effect of increased temperature on the 22 nm FD-SOI MOSFET devices' RF and mm-wave performance metrics (FoMs) of 22 nm FDSOI MOSFETs are presented through on-wafer measurements and extractions.

There is very limited literature on the performance of 22 nm FD-SOI devices at high temperatures. To the authors' best knowledge, the only work [3] studied mainly high frequency performance of FETs in this technology with limited data versus temperature. In our work, the existing study is extended by including detailed results of variation of various FoMs of FETs in this technology versus temperatures up to 175 °C.

## II. EXPERIMENTAL DETAILS

The devices used in this study are NFETs which originate from the 22 nm FD-SOI technology from GlobalFoundries [1]. The gate length is 20 nm, total width is 60  $\mu\text{m}$  for each of these devices composed of 120 fingers (20 fingers with a multiplicity of 6) of 0.5  $\mu\text{m}$  finger width.

For the RF characterization, S-parameters are measured in a frequency range from 200 MHz to 40 GHz. A PNA-X vector network analyser and two RF  $|Z|$  probes of 100  $\mu\text{m}$  pitch are used for these measurements. SOLT (Short-open-load-thru) method is used for calibration at each temperature point separately. De-embedding is done by measuring dedicated Open and Short structures corresponding to each device. The temperature points at which measurements have been carried out are 25 °C, 75 °C,

125 °C and 175 °C respectively. This has been achieved by using a Thermochuck from Temptronic that allows heating up the devices to the desired temperature points with accurate and stable temperature control. The system was kept steady for 30 minutes on reaching each temperature point to aid in stabilizing the temperature of the devices and calibration kit. The back gate was grounded during measurements ( $V_{bg} = 0$  V).

### III. RESULTS AND DISCUSSION

Fig. 1 shows the  $I_d$ - $V_g$  and the  $g_m$ - $V_g$  curves in saturation at  $V_d = 0.8$  V at the 4 different temperature points. The Zero Temperature Coefficient (ZTC) point for  $I_d$ , defined as the  $V_g$  at which  $I_d$  remains the same regardless of temperature, is observed to be at a  $V_g$  around of 0.62 V (for  $V_d = 0.8$  V).  $I_d$  increases with temperature at lower  $V_g$  biases, because of reduction in threshold voltage with increasing temperature. However,  $I_d$  decreases with increasing temperature at higher  $V_g$  biases due to stronger phonon scattering decreasing carrier mobility. These two mechanisms balance each other at the ZTC point resulting in an  $I_d$  independent of temperature [4], [5]. A similar ZTC point for transconductance  $g_m$  is observed for  $V_g$  around 0.38 V, where the  $g_m$  remains constant regardless of temperature. Such a bias point could be of great interest for applications where  $g_m$  is required to be independent of temperature. With  $f_T$  being proportional to  $g_m$ , this also relates to a ZTC in  $f_T$  (where  $f_T$  does not change with temperature) at that corresponding ZTC point for  $g_m$  provided that the total gate capacitance  $C_{gg,T}$  is relatively independent of temperature as observed in (1).

$$f_T, f_{max} \sim \frac{g_{m,e}}{C_{gg,T}} \quad (1)$$

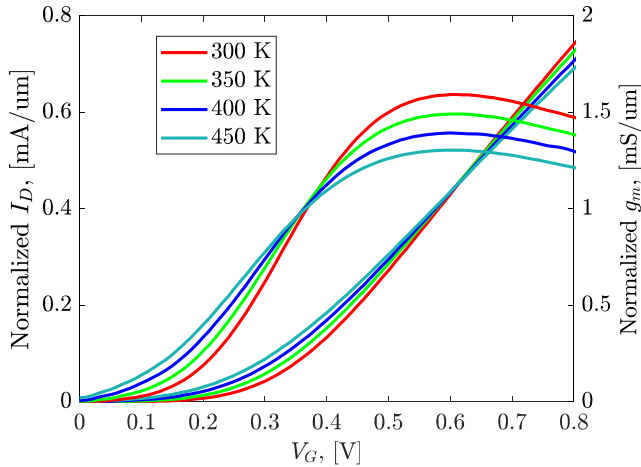


Fig. 1. Normalized drain current  $I_d$  and transconductance  $g_m$  vs gate voltage  $V_g$  at  $V_d = 0.8$  V at different temperatures.

The reduction of threshold voltage  $V_{Th}$  with temperature is shown in Fig. 2. The  $V_{Th}$  shown here is computed using the second-derivative method from [6] in the linear regime.  $V_{Th}$  reduction per unit temperature is found to be 0.6 mV/°C from the measurements over the temperature range of 300 K to 450 K. Such a  $V_{Th}$  reduction slope with temperature is a typical value observed in advanced technologies with ultra-thin bodies like UTBB, FinFETs, nanowires etc [7].

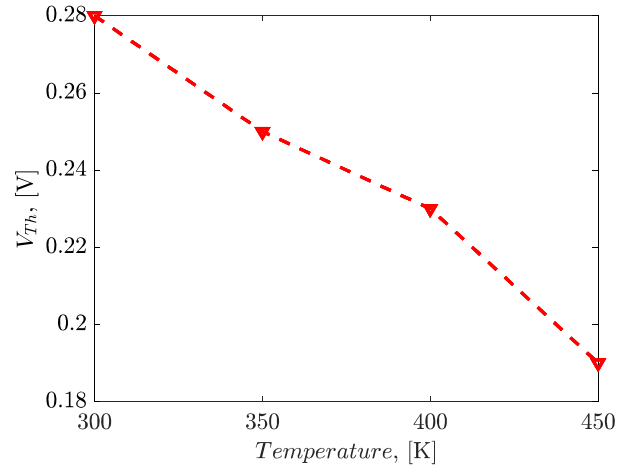


Fig. 2.  $V_{Th}$  variation versus temperature.

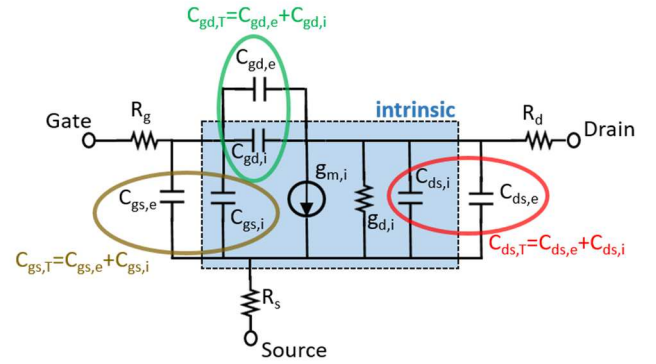


Fig. 3. Small signal equivalent circuit for MOSFET [10].

Regarding the extraction, from the RF measurements, the S-Parameters are converted into Y-parameters. The output conductance ( $g_d$ ) is computed as the real part of  $Y_{dd}$ , transconductance ( $g_m$ ) is the real part of  $Y_{dg}$ . The capacitances can be computed from the imaginary part of Y-parameters. The small signal equivalent circuit (SSEC) for MOSFETs can be represented as shown in Fig. 3. The SSEC elements can be extracted from the S-parameter measurements similar to the procedure described in [11]. Extrinsic parameters refer to the measured values whereas intrinsic parameters refer to the case where the parasitics are removed. Thus, extrinsic parameters  $g_{m,e}$ ,  $C_{gd,e}$ ,  $C_{gs,e}$  and  $C_{ds,e}$  refer to the measured transconductance, gate-to-drain capacitance, gate-to-source capacitance and drain-to-source capacitance respectively, while  $g_{m,i}$ ,  $C_{gd,i}$ ,  $C_{gs,i}$  and  $C_{ds,i}$  represent their intrinsic counterparts.  $R_g$ ,  $R_d$  and  $R_s$  are the gate, drain and source resistances respectively. In this paper, we focus on the transconductance  $g_m$  and the total gate capacitance  $C_{gg,T}$  without going into details of the other SSEC elements. Their effect on  $f_T$  and  $f_{max}$  are discussed. The values of parameters demonstrated in this work are normalized with respect to the total width of the device.

Both the maximum intrinsic and extrinsic transconductances  $g_{m,i}$  and  $g_{m,e}$  show a degradation of around 24% and 18% going from 300 K to 450 K respectively, as

demonstrated in Fig. 4. The bias condition was  $V_d = 0.8$  V and  $V_g = 0.6$  V (the value of  $V_g$  for which  $g_{m,max}$  was observed). The degradation in  $g_{m,e}$  is related to both  $R_{sd}$  variation and mobility degradation with temperature whereas the degradation in  $g_{m,i}$  is related to mobility degradation only. As  $R_{sd}$  variation is weaker than that of mobility, the degradation in  $g_{m,i}$  is stronger than that of  $g_{m,e}$ .

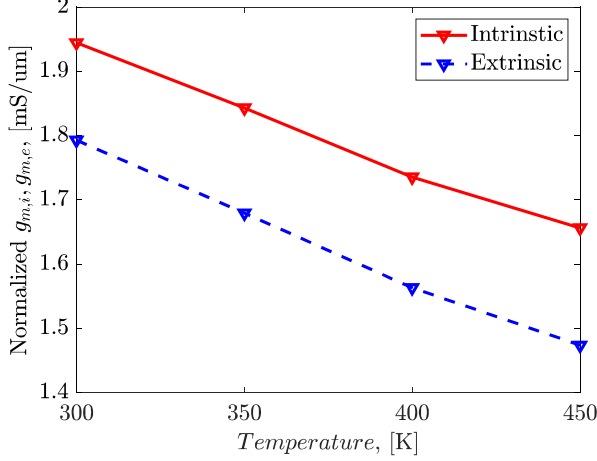


Fig. 4. Variation of maximum normalized intrinsic and extrinsic transconductance  $g_{m,i}$  and  $g_{m,e}$  with temperature at  $V_d = 0.8$  V and  $V_g$  corresponding to  $g_{m,max}$ .

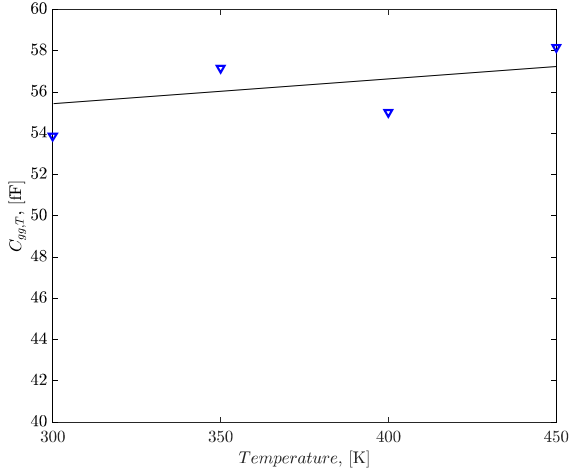


Fig. 5. Variation of total gate capacitance  $C_{gg,T}$  with temperature at  $V_g = V_d = 0.8$  V.

In Fig. 5, the variation of total gate capacitance  $C_{gg,T}$  versus temperature is demonstrated.  $C_{gg,T}$  extracted is found to be mostly steady over the temperature range of 300 to 450 K, varying by only a few fF which is within the extraction precision.

Two of the main parameters of interest, the RF FoMs, the  $f_T$  and  $f_{max}$  are found to degrade with temperature as seen in Fig. 6 and Fig. 7 respectively.  $f_T$  and  $f_{max}$  are computed from the extrapolation of the current gain  $H_{21}$  and unilateral gain to 0 dB respectively at  $V_d = 0.8$  V and  $V_g = 0.6$  V (that corresponds to maximum  $g_m$ ). Qualitatively, referring back to (1),  $f_T$  is proportional to  $g_{m,e}$ . This is seen from the trends observed in

Fig. 6 for  $f_T$  as  $f_T$  degrades in a similar manner to  $g_m$  as expected. Following up from this,  $f_{max}$  is seen to be degrading with temperature as well. On going from room temperature to 450 K, a reduction of 22% and 14% can be observed for  $f_T$  and  $f_{max}$  respectively.

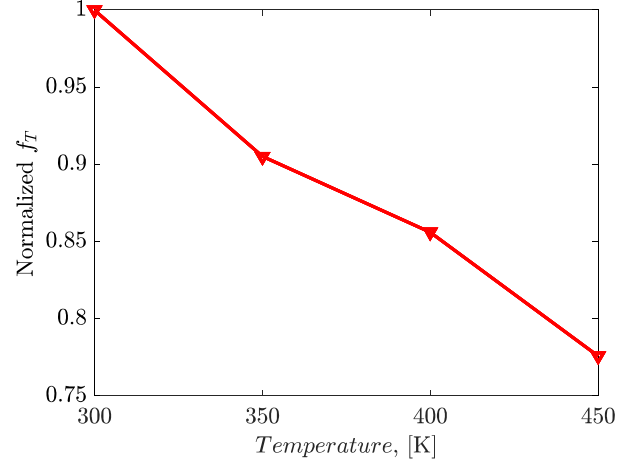


Fig. 6. Variation of normalized current-gain cut-off frequency  $f_T$  with temperature at  $V_d = 0.8$  V and  $V_g$  corresponding to  $g_{m,max}$ .

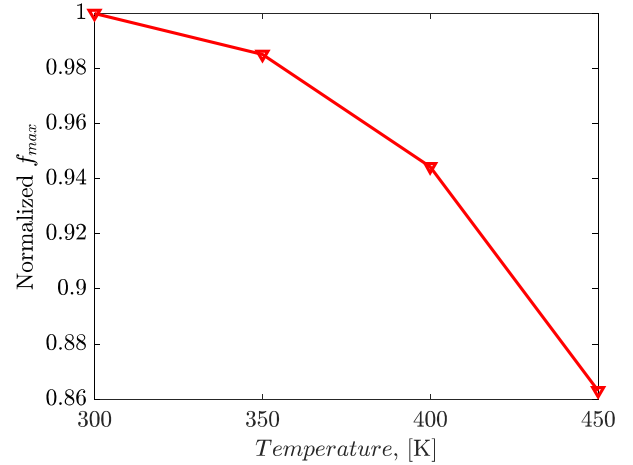


Fig. 7. Variation of normalized maximum oscillation frequency  $f_{max}$  with temperature at  $V_d = 0.8$  V and  $V_g$  corresponding to  $g_{m,max}$ .

#### IV. CONCLUSION

The effect of temperature rise on the RF FoMs from measurements of MOSFETs in 22 nm FDSOI technology was studied in this work. The ZTC points for  $I_d$  and  $g_m$  were observed from the IV characteristics with temperature.  $V_{Th}$  was seen to reduce by 0.6 mV/ $^{\circ}$ C over the temperature range of 300 to 450 K. For the RF FoMs, around 21% reduction in  $f_T$  and 14% reduction in  $f_{max}$  was observed when temperature is increased from 300 K to 450 K. Additionally, the behaviour of transconductance  $g_m$  and gate capacitance  $C_{gg}$  with temperature was also investigated. The degradation in  $g_m$  with temperature was found to be one of the major factors for the reduction in the aforementioned FoMs.

## ACKNOWLEDGMENT

This work is supported by Ecsel JU project "Beyond5" (grant agreement No. 876124) via EU H2020 and Innoviris (Brussels/Belgium) funding. The authors would like to thank GlobalFoundries for chip fabrication and their research support. The authors also express their gratitude for Pascal Simon from WELCOME characterization facility at Université catholique de Louvain for his assistance and support in the measurement setup.

## REFERENCES

- [1] S. N. Ong et al., "A 22nm FDSOI Technology Optimized for RF/mmWave Applications," 2018 IEEE Radio Frequency Integrated Circuits Symposium (RFIC), 2018, pp. 72-75.
- [2] R. W. Johnson et al., "The changing automotive environment: high-temperature electronics," in IEEE Transactions on Electronics Packaging Manufacturing, vol. 27, no. 3, pp. 164-176, July 2004.
- [3] M. Sadegh Dadash et al., "DC-170 GHz Characterization of 22nm FDSOI Technology for Radar Sensor Applications," 2018 13th European Microwave Integrated Circuits Conference (EuMIC), 2018, pp. 158-161, doi: 10.23919/EuMIC.2018.8539934.
- [4] J. -. Eggermont et al., "Design of SOI CMOS operational amplifiers for applications up to 300/spl deg/C," in IEEE Journal of Solid-State Circuits, vol. 31, no. 2, pp. 179-186, Feb. 1996, doi: 10.1109/4.487994.
- [5] L. Nyssens et al., "On the Separate Extraction of Self-Heating and Substrate Effects in FD-SOI MOSFET," in IEEE Electron Device Letters, vol. 42, no. 5, pp. 665-668, May 2021.
- [6] H. S. Wong et al., "Modeling of transconductance degradation and extraction of threshold voltage in thin oxide MOSFET," Solid State Electron., vol. 30, no. 9, pp. 953-968, Sep. 1987.
- [7] V. Kilchytska et al., "Ultra-thin body and thin-BOX SOI CMOS Technology Analog Figures of Merit", Solid State Electronics, vol. 70, pp.50-58, 2012. online 2011, doi:10.1016/j.sse.2011.11.020.
- [8] V. Kilchytska et al., "Trigate nanowire MOSFETs analog figures of merit". Solid-State Electronics, 7., 2015.
- [9] V. Kilchytska et al., "Specific features of multiple-gate MOSFET threshold voltage and subthreshold slope behavior at high temperatures", Solid State Electronics, Vol. 51, No. 9, pp 1185-1193, 2007.
- [10] L. Nyssens et al., "28-nm FD-SOI CMOS RF Figures of Merit Down to 4.2 K," in IEEE Journal of the Electron Devices Society, vol. 8, pp. 646-654, 2020, doi: 10.1109/JEDS.2020.3002201.
- [11] B. Kazemi Esfeh et al., "Assessment of 28 nm UTBB FD-SOI Technology Platform for RF Applications: Figures of Merit and Effect of Parasitic Elements," in *Solid-State Electronics*, vol. 117, pp. 130-37, 2016.